

Compact SOI-based polarization diversity wavelength de-multiplexer circuit using two symmetric AWGs

S. Pathak,^{*1} M. Vanslembrouck,¹ P. Dumon,¹ D. Van Thourhout,¹ and W. Bogaerts¹

¹Photonics Research Group (INTEC), Ghent University - imec,
Sint-Pietersnieuwstraat 41,
B-9000 Ghent, Belgium

[*Shibnath.Pathak@intec.UGent.be](mailto:Shibnath.Pathak@intec.UGent.be)

Abstract: We demonstrate a compact 16-channel 200GHz polarization diversity wavelength de-multiplexer circuit using two silicon AWGs and 2D grating couplers. Estimated fiber to fiber loss is better than -15.0dB . Insertion loss and crosstalk induced by the AWGs are -2.6dB and 21.5dB , respectively. The maximum polarization dependent wavelength shift is 0.12nm . The polarization dependent loss varies between 0.06dB and 2.32dB over the 16 channels. The total circuit footprint is $1400 \times 850\mu\text{m}^2$.

© 2012 Optical Society of America

OCIS codes: (130.0130) Integrated optics; (130.1750) Components; (130.7408) Wavelength filtering devices; (130.3120) Integrated optics devices.

References and links

1. M. Smit and C. Van Dam, "PHASAR-based WDM-devices: principles, design and applications," *IEEE J. Selected Topics in Quantum Electron.* **2**(2), 236–250 (1996).
2. W. Bogaerts, S. Selvaraja, P. Dumon, J. Brouckaert, K. De Vos, D. Van Thourhout, and R. Baets, "Silicon-on-insulator spectral filters fabricated with CMOS technology," *IEEE J. Selected Topics in Quantum Electron.* **16**(1), 33–44 (2010).
3. A. Himeno, K. Kato, and T. Miya, "Silica-based planar lightwave circuits," *IEEE J. Selected Topics in Quantum Electron.* **4**(6), 913–924 (1998).
4. M. Kohtoku, H. Sanjoh, S. Oku, Y. Kadota, Y. Yoshikuni, and Y. Shibata, "InP-based 64-channel arrayed waveguide grating with 50 GHz channel spacing and up to -20 dB crosstalk," *Electron. Lett.* **33**, 1786–1787 (1997).
5. Q. Fang, T.Y. Liow, J. F. Song, K. W. Ang, M. B. Yu, G. Q. Lo, and D.L. Kwong, "WDM multi-channel silicon photonic receiver with 320 Gbps data transmission capability," *Opt. Express* **18**(5), 5106–5113 (2010).
6. S. K. Selvaraja, W. Bogaerts, and D. Van Thourhout, "Loss reduction in silicon nanophotonic waveguide microbends through etch profile improvement," *Opt. Commun.* **284**(8), 2141–2144 (2011).
7. C. Doerr, M. Zirngibl, C. Joyner, L. Stulz, and H. Presby, "Polarization diversity waveguide grating receiver with integrated optical preamplifiers," *IEEE Photon. Tech. Lett.* **9**(1), 85–87 (1997).
8. T. Barwicz, M. R. Watts, M. A. Popović, P. T. Rakich, L. Socci, F. X. Kärtner, E. P. Ippen, and H. I. Smith, "Polarization-transparent microphotonic devices in the strong confinement limit," *Nat. Photonics* **1**(1), 57–60 (2007).
9. W. Bogaerts, D. Taillaert, P. Dumon, D. Van Thourhout, R. Baets, and E. Pluk, "A polarization-diversity wavelength duplexer circuit in silicon-on-insulator photonic wires," *Opt. Express* **15**(4), 1567–1578 (2007).
10. D. Taillaert, F. Van Laere, M. Ayre, W. Bogaerts, D. Van Thourhout, P. Bienstman, and R. Baets, "Grating couplers for coupling between optical fibers and nanophotonic waveguides," *Japanese J. Appl. Phys.* **45**(8A), 6071–6077 (2006).
11. M. Pu, L. Liu, H. Ou, K. Yvind, and J. r. M. Hvam, "Ultra-low-loss inverted taper coupler for silicon-on-insulator ridge waveguide," *Opt. Commun.* **283**(19), 3678–3682 (2010).
12. W. Bogaerts, P. Dumon, D. V. Thourhout, D. Taillaert, P. Jaenen, J. Wouters, S. Beckx, V. Wiaux, and R. G. Baets, "Compact wavelength-selective functions in silicon-on-insulator photonic wires," *IEEE J. Selected Topics in Quantum Electron.* **12**(6), 1394–1401 (2006).

13. D. Taillaert, H. Chong, and P. Borel, "A compact two-dimensional grating coupler used as a polarization splitter," *IEEE Photon. Tech. Lett.* **15**(9), 1249–1251 (2003).
14. F. Van Laere, W. Bogaerts, P. Dumon, G. Roelkens, D. Van Thourhout, and R. Baets, "Focusing polarization diversity grating couplers in silicon-on-insulator," *IEEE J. Lightwave Tech.* **27**(5), 612–618 (2009).
15. T. Fukazawa, F. Ohno, and T. Baba, "Very compact arrayed waveguide grating demultiplexer using Si photonic wire waveguides," *Japanese J. Appl. Phys.* **43**(5B), L673–L675 (2004).
16. S. Pathak, E. Lambert, P. Dumon, D. Van Thourhout, and W. Bogaerts, "Compact SOI-based AWG with flattened spectral response using a MMI," in *IEEE International Conference on Group IV Photonics (Institute of Electrical and Electronics Engineers, London, 2011)*, pp. 45–47.
17. R. Halir, D. Vermeulen, and G. Roelkens, "Reducing polarization-dependent loss of silicon-on-insulator fiber to chip grating couplers," *IEEE Photon. Tech. Lett.* **22**(6), 389–391 (2010).
18. S. Pathak, M. Vanslebrouck, P. Dumon, D. Van Thourhout, and W. Bogaerts, "Compact SOI-Based polarization diversity wavelength de-multiplexer circuit using two symmetric AWGs," in *European Conference and Exhibition on Optical Communication (Optical Society of America, Netherlands, 2012)*.

1. Introduction

High contrast silicon-on-insulator (SOI) waveguides have gained popularity for photonics integrated circuits because of their compatibility with CMOS technologies. The sub-micron SOI waveguides and the sharp bends allow very compact components, which gives more flexibility to integrate many optical functions on a single chip. One such compact component in SOI is the arrayed waveguide grating (AWG) [1, 2], which is commonly used for wavelength division multiplexing (WDM) in telecoms networks. Highly confined silicon waveguides allow a significant reduction in footprint of AWGs compared to traditional low-contrast waveguide platforms [3–5]. But the high contrast waveguides severely impact on the performance of the AWGs: sidewall roughness introduces losses, as well as phase errors in the delay lines, and similarly, silicon thickness variations can affect the dispersion and therefore the intended channel spacing. Some of these problems are solved by improving the fabrication process [6] while others are addressed by modifying the designs and making them more tolerant [2].

In addition to that, silicon high contrast waveguides are strongly polarization sensitive. As a

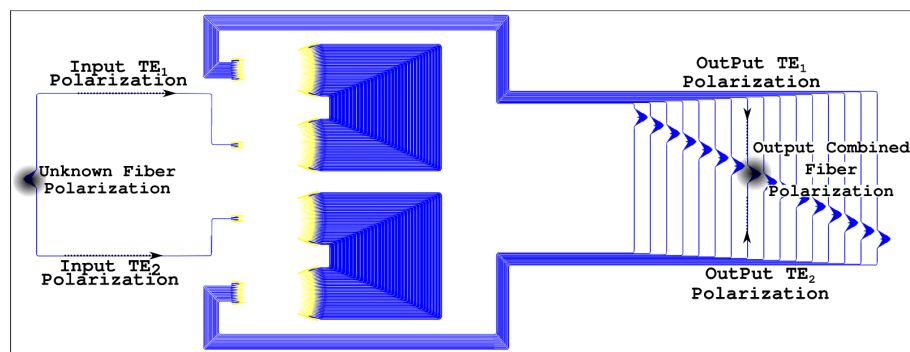


Fig. 1. Schematic diagram of $16 \times 400\text{GHz}$ Polarization diversity circuit.

result devices like AWGs inherently become polarization dependent. So one of the limitations of SOI AWGs is that they work only for a single polarization. This is difficult to combine with inputs from standard single-mode fibers with an unknown and variable polarization state. Because polarization-independent waveguides in high-contrast silicon are difficult to make, the commonly accepted approach to achieve a polarization independent circuit is the polarization diversity scheme [7, 8]: incoming signals with unknown polarization are split into two orthogonal polarizations which are then coupled separately in two identical single-polarization circuits

as shown in Fig. 1. The key challenge for this scheme to work is to realize two completely identical circuits, requiring a highly accurate fabrication process or active tuning or trimming. In some cases, the polarization diversity circuit with two AWGs can be replaced by a single AWG used in both directions [9]. But this is not always possible and introduces additional loss and back reflection in the fiber. Therefore, in this paper we demonstrate a compact SOI-based polarization diversity wavelength de-multiplexer circuit using two symmetric AWGs and a compact 2-D grating coupler, which is used to couple the unknown fiber polarization into two separate waveguides by splitting the light in two orthogonal polarizations.

2. Design of the 2D grating Coupler

There are a few commonly used techniques to couple light into or out of a silicon photonic circuit. These include vertical coupling using a grating coupler [10], and horizontal coupling using a mode converter [11]. In our SOI photonics circuit we use fiber grating couplers for both input and output. Depending on its design, and in particular its period, a typical 1-D fiber grating coupler will couple either the TE or the TM polarization into the waveguide. In most cases the TE polarization is targeted, as this is the ground mode of a standard sub-micron wire waveguide [12]. A 2-D fiber grating coupler can couple any fiber polarization by splitting them into the TE modes of two orthogonally oriented waveguides [13]. Vice versa, the 2-D grating coupler can couple the light back into the fiber by combining the two TE modes into orthogonal fiber modes. This splitter/combiner functionality of 2-D grating couplers allows us to drive

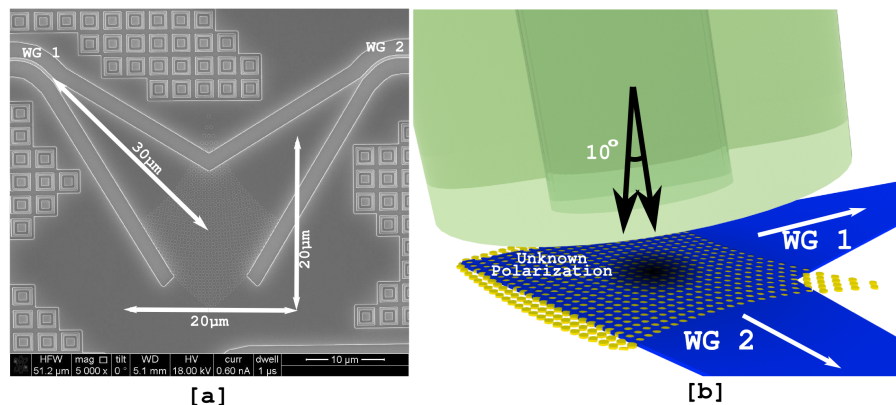


Fig. 2. (a) Fabricated 2D grating coupler. (b) Schematic diagram of a 2D grating coupler with fiber align.

two identical circuits separately to achieve polarization independent operation in a polarization diversity scheme. Figure 2(a) shows a SEM-picture and a schematic diagram of a 2-D focusing grating coupler. The use of the 2-D focusing grating coupler [14] reduces the taper length of the access waveguide compare to the standard 2-D grating coupler [13]. As shown in Fig. 2(b) the fiber is placed quasi vertically over the grating with a 10° tilt to avoid coupling to the backward propagating mode and reflections back into the fiber. The 2-D grating couplers are fabricated using a double etch process. The grating holes are etched 70nm into a 220nm thick silicon slab while the access waveguides are defined by etching 220nm deep trenches. The diameter of the grating holes is 390nm and the pitch of the grating is 610nm . The grating lines are curved to focus the coupled light directly into a 500nm wide wire waveguide within a distance of only $30\mu\text{m}$. This eliminates the need for a separate taper.

3. Design of the AWG

Due to its high index contrast which allows for tight bends, the silicon waveguide platform allows to design very compact arrayed waveguide grating devices [15, 16]. But the high contrast makes the waveguide also very sensitive to phase errors, and as a result a typical SOI AWG has higher crosstalk compared to AWGs fabricated in lower index contrast material systems. To alleviate this problem, a double etch process is used for fabricating the AWG [2] as shown in

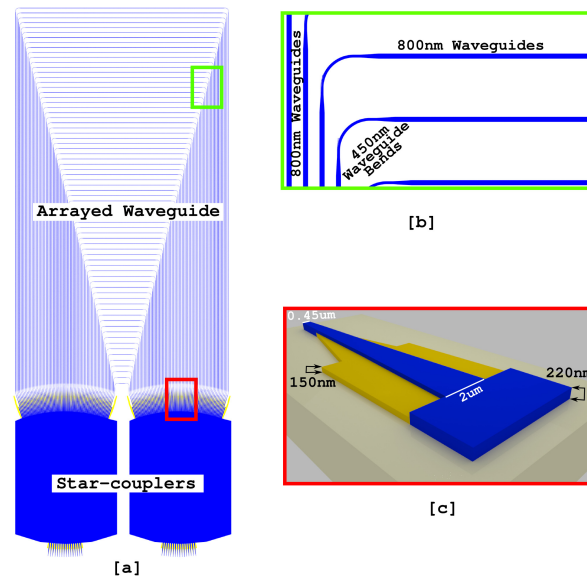


Fig. 3. (a) Mask layout of silicon AWG. (b) Zoom into waveguide array region, showing combination of 450nm and 800nm wide waveguides to minimize phase errors. (c) A $2\mu\text{m}$ wide shallow etched aperture.

Fig. 3. For defining the access waveguides and the bends in the waveguide array we use a deep etch (220nm) while for the apertures of the star couplers and the waveguide array itself we use a 70nm shallow etch. To further reduce the phase errors, mainly caused by the sidewall roughness of the waveguides, we use broad 800nm wide waveguides instead of 450nm wide single mode waveguides in the waveguide array as shown in Fig. 3(b). To avoid mode mixing inside the 800nm wide waveguides, they are tapered down to 450nm in the bends. In the star coupler we used $2\mu\text{m}$ wide apertures, which are fabricated by defining a 70nm etched trench, as shown in the Fig. 3(c). These 70nm etched apertures help to reduce the reflection from the interface with the free propagation region of the star coupler. We designed two 16 channels AWGs with 72 waveguides in the waveguide array as the basis of our polarization diversity circuit. The channel spacing is $200\text{GHz}(1.6\text{nm})$. The size of a single $16 \times 200\text{GHz}$ AWG (shown in Fig. 3(a)) is $365 \times 650\mu\text{m}^2$.

4. Measurement

To compare the performance of both AWG's forming the polarization diversity circuit we excited them separately by controlling the input polarization using an external electronic polarization controller (HP8169A). We use a known 1-D TE grating coupler to calibrate the fiber polarization. We align our fiber with respect to the grating using a X-Y-Z moveable stage by actively maximizing the transmitted power. A fully automatic setup which allows us to align

the fiber with an accuracy of $0.01\mu\text{m}$ is used.

5. Analysis of the 2D grating coupler

To analyze the performance of the 2D grating coupler we designed a test circuit where 2D grating couplers are directly connected with two 1D grating couplers which only couple the TE polarization of the waveguide. We excited the 2D grating coupler with four differently oriented fiber polarizations (90, -45, 0 and 45 degree with respect to the axis of the 2D grating, respectively denoted as *Pol-1*, *Pol-2*, *Pol-3*, and *Pol-4* in Fig. 4) and measured the spectral

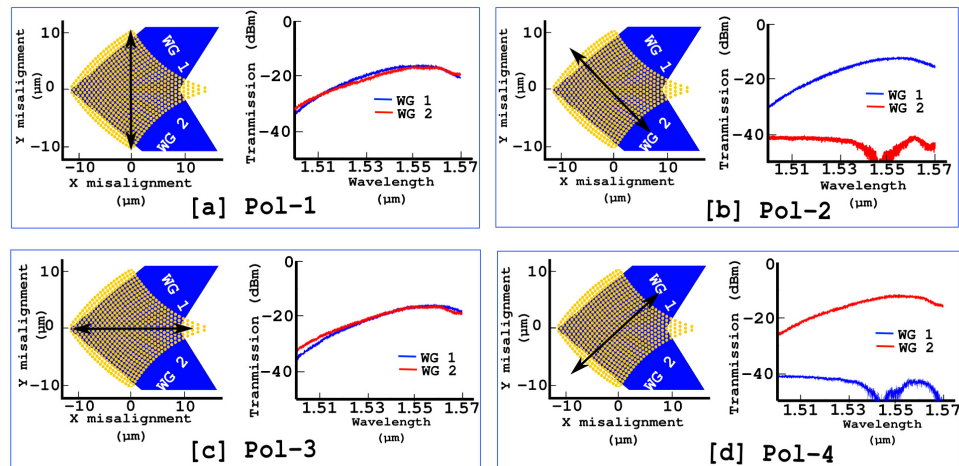


Fig. 4. Spectral response of a 2D grating coupler connected to two 1D grating couplers for differently oriented input polarizations ((a) *Pol-1*: 90 degree, (b) *Pol-2*: -45 degree, (c) *Pol-3*: 0 degree, (d) *Pol-4*: 45 degree oriented fiber polarizations with respect to the axis of the 2D grating).

response from two waveguides connected to the 2D coupler and terminated with 1D TE grating couplers (which are denoted as *WG-1* and *WG-2* in Fig. 4). Figure 4 shows that when the 2D grating coupler is excited by the 90 or 0 degree oriented polarization (*Pol-1* and *Pol-3*) the power is divided equally into both waveguides (*WG-1* and *WG-2*). To the contrary, when the polarization is oriented along the -45 or 45 direction, the light predominantly couples towards respectively *WG-1* and *WG-2* as we can see in Fig. 4(b) and 4(d). Figure 4 also shows that the transmission is wavelength dependent, which is related to the wavelength dependent coupling efficiency of the 1D and 2D grating couplers.

Using our automatic setup, we mapped the tolerance towards fiber misalignments of the 2-D grating coupler. The input fiber was scanned over the grating coupler in a 2-D pattern, while the output fiber was fixed at its original position above the 1D grating couplers connected to respectively *WG-1* and *WG-2*. The center between the two positions obtained by optimizing the transmission through respectively *WG-1* and *WG-2* with the input polarization oriented along *Pol-3* was taken as the origin (0, 0) for plotting Fig. 5. The mapping was carried out for a wavelength of $1.55\mu\text{m}$. From Fig. 5 we can observe that an equal amount of power is coupled to *WG-1* and *WG-2* for the polarization oriented along *Pol-1* and *Pol-3*, when shifting their maximum transmission position towards the respective waveguides. For polarization *Pol-2* and *Pol-4* the maximum transmission position shifts towards the waveguide *WG-1* and *WG-2*, respectively. The offset between the optimal position of *WG-1* and *WG-2* is less

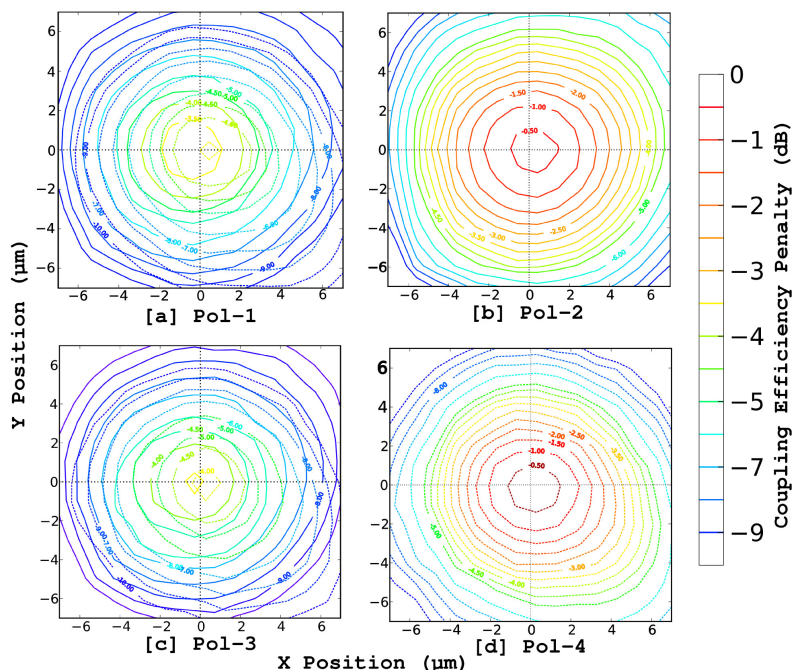


Fig. 5. Mapping of alignment tolerance for different oriented fiber polarizations ((a) Pol-1: 90 degree, (b) Pol-2: -45 degree, c) Pol-3: 0 degree, (d) Pol-4: 45 degree oriented fiber polarizations with respect to the axis of the 2D grating). (a) and (c) The solid line represents the transmission through waveguide $WG-1$. The dashed line represent the transmission through waveguide $WG-2$.

than a micrometer and similarly, the offset between the maximum transmission positions for polarization $Pol-2$ and $Pol-4$ is less than half micrometer. These offsets in optimal coupling positions are the main source of the polarization dependent loss (PDL) in this circuit. It is also possible to optimize the alignment of the fiber for maximum overlap of the spectrums to reduce the PDL. But this will introduce an additional insertion loss. From Fig. 5 we can also observe that the power drops by $2dB$ if the fiber moves $4\mu m$ away from the center. The PDL of the 2D grating coupler can be further improve by using a π phase-shifter at one of the waveguide [17].

To evaluate the wavelength dependent transmission for light polarized along $Pol-1$ and $Pol-3$ we use a reference circuit where by two 2D grating couplers are connected with two equal length waveguides. We optimize the alignment of both fibers for the $Pol-1$ polarization and measure the spectral response for both the $Pol-1$ and $Pol-3$ polarizations. The results are shown in Fig. 6(a). Both spectra are shifted with respect to each other. This is the main origin of polarization dependent loss in our polarization diversity circuits. In Fig. 6(b) shows the wavelength range where the spectral response of the 2D grating becomes nearly flat. In this range the wavelength variation of the PDL is minimal compare to the rest of the spectrum. The measured PDL of the 2-D grating coupler is $1.1dB$ at the wavelength of $1.52\mu m$ where we measure the highest coupling efficiency.

6. Analysis of full Polarization Diversity Circuit

Figure 7 shows the spectral response of a 16 channel ($200GHz$ channel spacing) polarization diversity wavelength de-multiplexer circuit for $Pol-1$ and $Pol-3$ polarizations. The center

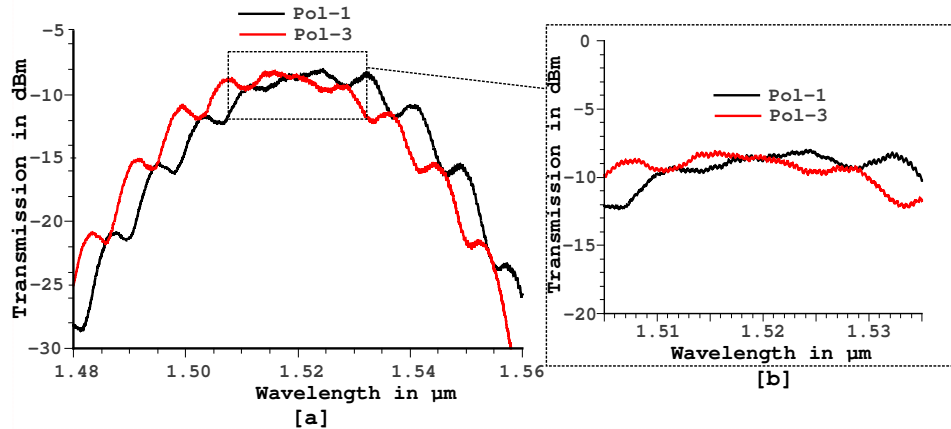


Fig. 6. Transmission of two 2-D grating couplers connected through waveguides. (a) Spectral response of the 2D grating for wavelength range of $1.48\mu\text{m}$ to $1.56\mu\text{m}$. (b) Flat passband spectral response of the 2D grating.

channel experience an on-chip insertion loss of -2.6dB [18] contributed by the AWGs. The estimated loss introduced by the two 2D grating couplers (one at input and other at the output) is 12dB . The crosstalk of the circuit is 21.5dB [18]. The output channels are well aligned in terms of polarization-dependent wavelength shift. From the Fig. 7 we can observe the power is well matched for channels 7, 8, 9, 13, 14 and 15 as the channels are laid on the overlapped wavelength region of the 2D grating couplers, shown in Fig. 6(b). The other channels are experienced power

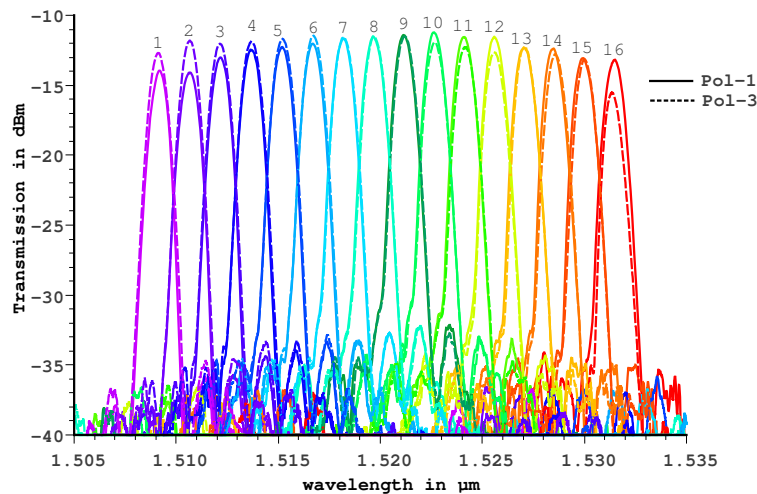


Fig. 7. Spectral response of a 16 channels 200GHz polarization diversity wavelength demultiplexer circuit for $\text{Pol} - 1$ and $\text{Pol} - 3$ polarizations.

deviation due to the 2D grating coupler. The polarization-dependent loss is measured to be between 0.06dB (channel 8) and 2.32dB (channel 16) in the worst respectively best case.

The mismatch between the two fabricated AWGs induces a polarization-dependent wavelength shift, but is very low, as can be seen in Fig. 7. Figure 8(a) plots the position of all 16 channels for the four polarization states considered. The polarization-dependent wavelength

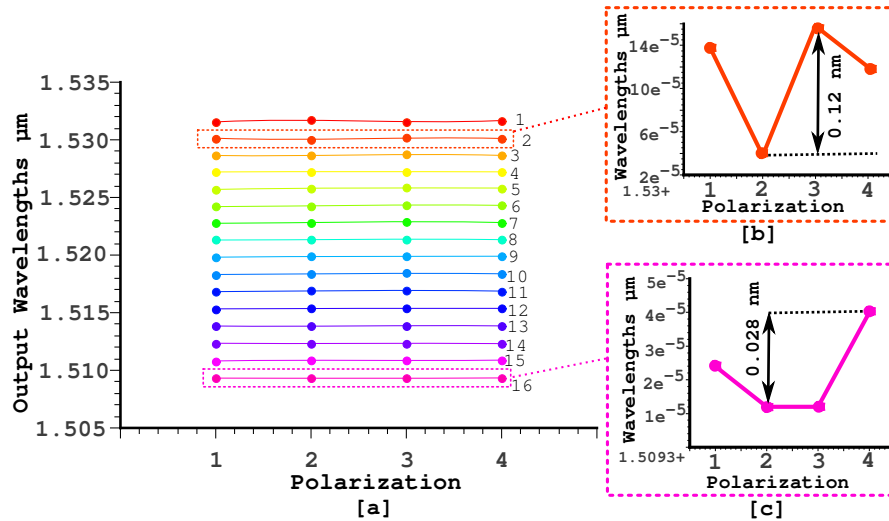


Fig. 8. (a) The output wavelength channel positions of the polarization diversity circuit for *Pol* – 1, *Pol* – 2, *Pol* – 3, and *Pol* – 4 polarizations. (b) Maximum shifted output channel. (c) Minimum shifted output channel.

shift is measured to be between 0.12nm and 0.028nm in the worst respectively best case, as shown in Fig. 8(b) and 8(c).

7. Conclusion

We demonstrate a $16 \times 200\text{GHz}$ polarization diversity wavelength de-multiplexer circuit integrated on an SOI platform. Estimated fiber to fiber loss is better than -15.0dB . Insertion loss and crosstalk induced by the AWGs are -2.6dB and 21.5dB , respectively. The polarization dependent loss varies between 0.06dB and 2.32dB over the 16 channels. The polarization dependent wavelength shift varies between 0.12nm and 0.028nm over the 16 channels. The total circuit size is $1400 \times 850\mu\text{m}^2$.

Acknowledgment

This work was supported by the European Union in the framework of the FP7-project ICT-HELIOS and the ERC-projects INSPECTRA and ULPPIC.